

# FAST SCANNING DIAMOND DETECTOR FOR ELECTRON BEAM PROFILE MONITORING\*

V. V. Konovalov<sup>†</sup>, Applied Diamond, Inc., Wilmington, DE, USA  
T. Miller, S. Bellavia, C. Brutus, P. Thieberger, and R. Michnoff,  
Brookhaven National Laboratory, Upton, NY, USA

## Abstract

The first prototype of a fast scanning diamond beam profile detector (DBPD) suitable for invasive high power CW electron beam core profile measurements in transmittance mode was developed. It consists of a multi-strip solid state diamond detector to scan with high speed (up to 1 m/s) and precision (about 5  $\mu\text{m}$ ) through the core of an electron beam. The diamond sensor was made from a thin polycrystalline diamond (PCD) plate with highly B-doped diamond conductive strips both grown by CVD. Transient currents from the multi-strip detector were measured with fast digitizing electrometers. Successful operation of the DBPD was demonstrated for pulsed (5 Hz) and CW (78 kHz) CeC beams, including the detector's ability to withstand a 20 sec insertion into the CW CeC beam core. The X-Y beam spatial profile was measured in one scan. Thermal modelling demonstrated a manageable thermal impact even from a relatively long insertion of the diamond sensor into the CW CeC core and very short (0.2 s) insertion into the CW LEReC beam core. Electrical impedance modelling of the detector and vacuum chamber assembly demonstrated minimal impact on beam line impedance with diamond sensor insertion.

## INTRODUCTION

Recently, novel electron cooling systems for ion beams are being developed at Brookhaven National Laboratory, such as the Low Energy electron Cooling (LEReC) system, the first electron cooler without any magnetization, designed to maximize collision rates at the lowest energies available at the Relativistic Ion Collider (RHIC) [1], and the ongoing Coherent electron Cooling (CeC) Proof of Principle (CeC PoP) experiment, currently installed in the RHIC tunnel [2]. LEReC system produces 704 MHz electron bunches, modulated at 9 MHz to overlap Au-ion bunches, with 1.6 - 2.6 MeV electron energies and the beam power ranging from 10 to 140 kW. In the CeC experiment, the electron beam is produced by an electron gun followed by superconducting cavity and a 704 MHz superconducting LINAC producing a 15 MeV electron beam at up to 78 kHz repetition rate.

Efficient electron cooling requires a high quality, high power electron beam with tight parameters (energy and space trajectory). In order to achieve and maintain the required parameters and stability of the electron beam, its parameters have to be continuously monitored and feedback

control has to be developed [3]. Interference of beam diagnostic instrumentation with the beam may lead to degradation of beam parameters therefore, invasive and non-interceptive methods of monitoring are preferred. Invasive beam monitoring can be achieved by using highly transparent detectors made from low-Z materials absorbing  $< 1\%$  of beam energy. However, existing detectors, e.g. wire scanners, are not suitable for invasive profile measurements of powerful continuous wave (CW) electron beams. As a result, the beam profile of these beams is currently monitored in low repetition pulsed mode and assumed to remain the same in CW mode. Common wire scanners have a rather short life-time even when used for pulsed beam monitoring. Their very thin wires are easily overheated and burned, thus contaminating the beam pipe with debris.

Diamond's unique combination of material properties: low energy absorption, tremendous radiation tolerance, ability to dissipate significant heat load, and stability of electronic properties over a wide temperature range, makes it an ideal material for high energy applications. Diamond radiation detectors (DRD) have been used for detection of many types of radiation demonstrating fast time response, high radiation stability, and ability to operate at high temperatures without cooling. DRDs have much longer lifetimes compared to radiation detectors made from other materials like silicon or plastic. Also the signals from gas-filled ion chambers and silicon detectors saturate under high-flux conditions. DRDs are an established technology as beam condition monitors in the highest radiation areas of all Large Hadron Collider experiments [4]. DRDs are used as X-ray beam position monitors for multiple synchrotron radiation and free electron laser sources, including NSLS-II at BNL [5], SOLEIL [6], and CEA at Saclay [7]. DRD was been used with a powerful 90 W/mm<sup>2</sup> white X-ray beam and demonstrated 11 orders of magnitude flux linearity and stable response over an 18 month time period [8]. DRD for electron beam profile and halo monitoring was developed and successfully tested for the XFEL/SPring-8 as a part of a system to protect undulator permanent magnets from radiation damage [9].

The first prototype of a fast scanning diamond beam profile detector (DBPD) suitable for invasive high power CW electron beam core profile measurements in transmittance mode has been developed and fabricated. Its research and development in significant degree was focused on future installation into the high power CeC and LEReC beam-lines at BNL and the detector design was tailored to the corresponding BNL requirements. Numerical modeling demonstrated that the DBPD prototype is suitable for direct

\* Work supported by DOE SBIR under grant No. DE-SC0020498 (AD) and by BSA under DOE contract DE-AC02-98CH10886 (BNL).

<sup>†</sup> Email address: val@ddk.com.

Table 1: Electron Beam Parameters

Beam	Diamond thickness (μm)	Electron Energy (MeV)	dE/dx (MeV cm <sup>2</sup> /g)	Beam Current (μA)	Beam σ <sub>x</sub> (mm)	Beam σ <sub>y</sub> (mm)	Max absorbed power density (W/cm <sup>2</sup> )	Absorbed power (%)
CeC	100	15	1.741	78	3	3	8.38	0.41
LEReC	100	2	1.568	35500	2.64	8.55	95	2.75

core beam profile measurements of the powerful CW mode CeC and LEReC beamlines. The DBPD prototype has been tested at the ATF and CeC electron beamlines at BNL.

## DESIGN OF DIAMOND DETECTOR

The mechanical design of the DBPD is shown in Fig. 1 and includes a vacuum chamber and a high speed actuator. Existing pneumatic actuators may provide the required high speed, but they lack speed stability, positioning accuracy and reproducibility. We used the 1 m/s hard shaft motor driven actuator with bellows developed by Ultra High Vacuum Design. Testing of the actuator demonstrated good constant speed over 60 mm travel, only 0.42% speed variation at 1 m/s, and good repeatability. The actuator was equipped with a custom feedthrough with an embedded Cu rod and 12 SMB coaxial connectors. In the initial position the diamond sensor is fully retracted from the beam pipe and at the lowest travel position is fully inserted into the beam core near the center of cube, see Fig. 1.

The diamond sensor consisted of a 48x19x0.15 mm detector-grade PCD plate with embedded 10 vertical and one horizontal conductive strip-lines. Highly B<sup>+</sup>-doped CVD diamond layers were grown on both sides of the intrinsic PCD plate. Then, on one side the boron layer was masked and RIE/ICP etched to form the strip-lines. The PCD plate was then brazed to a tungsten carbide support attached to the Cu rod (19 mm diameter, 20 cm long). The massive Cu rod provided a good heat sink for the thin diamond sensor.

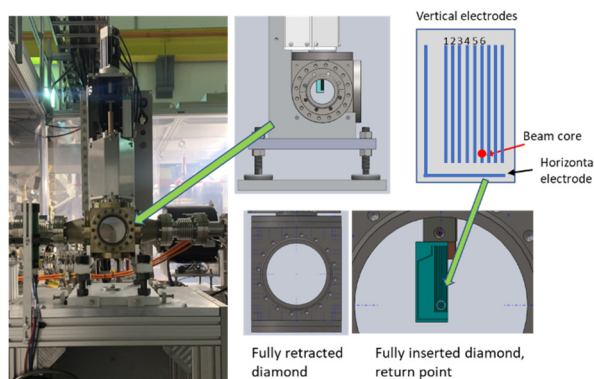


Figure 1: Diamond detector assembly installed at the CeC beam-line and its schematics.

## NUMERICAL MODELING

### Thermal Impact from High Power CW Electron Beams

Numerical modeling of the thermal impact on the diamond sensor from high power CW beams was performed

on a 3D mechanical model, see Fig. 2b, with ANSYS 2020 R1 software. The geometry of the diamond sensor was modeled with a fine element mesh (total 14,728 elements, comprised of 100,856 nodes). The modeling was performed for a number of cases: CeC and LEReC beams, normal and 45° tilted position of the diamond plate to the beam, static position and motion, and two types of metal substrates supporting the diamond sensor. Electron beam parameters and calculated absorbed beam energy are presented in Table 1, and material properties used in modeling are presented in Table 2.

Table 2: Material Properties

Material	Thermal Conductivity (W/m-K)	Density (kg/m <sup>3</sup> )	Specific Heat (J/kg-K)
PCD	1200	3515	502
WC-Co	49.6	15600	183
Copper	401	8300	385

### CeC Beam

Thermal modeling of a stationary and moving diamond sensor has been performed for CeC beam, see Fig. 2 for geometry and motion profile, corresponding to the maximum 1 m/s actuator speed and the stroke of 45 mm. Ambient temperature (25 C) was placed at the end of the copper rod further from detector. In stationary position sensor doesn't move and beam is turned on at zero time.

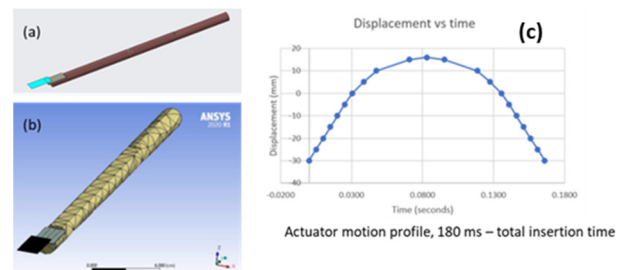


Figure 2: Geometry of diamond sensor brazed to the WC-Co and mounted on Cu rod (a), its fine element mesh (b), and motion profile of diamond sensor (c).

Temperature distribution for stationary sensor position is shown in Fig. 3 at 0.127 s after the beam was turned on and for the achieved steady state. The corresponding time dependence of the maximum temperature on the diamond is shown in Fig. 4. The steady state condition with maximum temperature of about 100 °C is reached at about 10-20 sec. The transient maximum temperature for the motion profile (see Fig. 2c) is shown in Fig. 5. The maximum temperature

Content from this work may be used under the terms of the CC BY 3.0 licence (© 2021). Any distribution of this work must maintain attribution to the author(s), title of the work, publisher, and DOI

of 30 °C occurs at about 40 ms and then within several seconds return to the ambient. The maximum steady state temperature for 45° tilted sensor was about 17 °C higher. The replacement of tungsten carbide support substrate to copper substrate, having the higher thermal conductivity, results in a small decrease of temperature by about 10 °C.

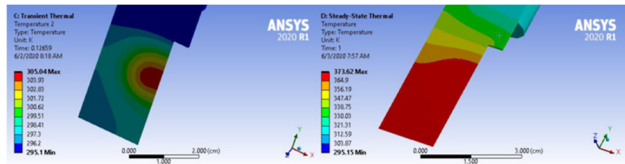


Figure 3: CeC beam, temperature profile at 0.127 s after the beam was turned on (left) and final steady state (right), beam normal orientation.

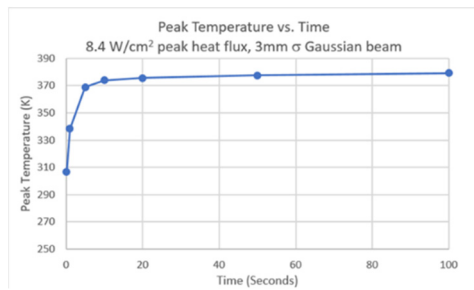


Figure 4: Maximum temperature time dependence after the beam was turned on.

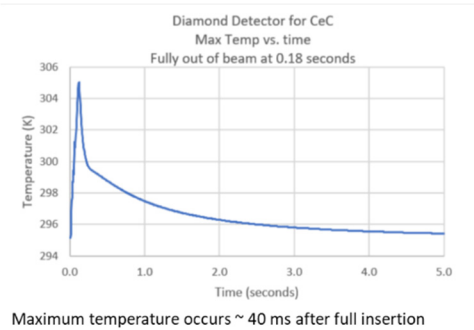


Figure 5: CeC beam, transient state with sensor motion. maximum temperature of diamond for the motion profile on Fig. 2c.

### LEReC Beam

The transient temperature profile for much more powerful LEReC beam was also calculated for the motion profile shown in Fig. 2c. The temperature map at short times is shown in Fig. 6 and the time dependence of maximum temperature is shown in Fig. 7. In this case of LEReC beam the maximum temperature of about 370 °C occurs at about 140 ms and then similarly to CeC returns to the ambient within 5 seconds.

### Electrical Response and Effect of Ferrite Addition

The vacuum chamber electrical response to the CeC beam was modeled using Particle Studio for the cases with and without additional ferrite installed into the vacuum chamber.

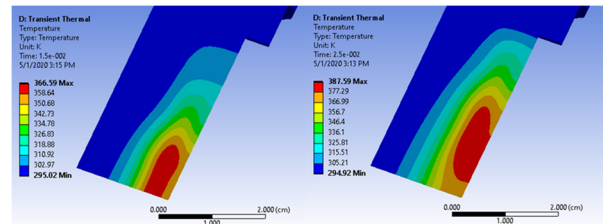


Figure 6: LEReC beam, temperature profile at 15 ms insertion time (left) and 25 ms time (right), beam normal orientation.

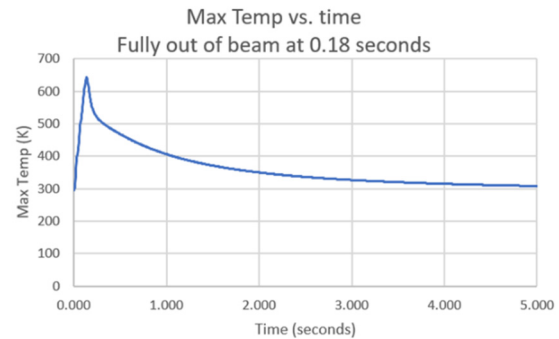


Figure 7: LEReC beam, transient state with sensor motion. Maximum temperature of diamond sensor for the motion profile in Fig. 2c.

amber. The results are shown on Fig. 8 and demonstrate that even one ferrite is very effective in attenuating the oscillations. The oscillations are not the wake field but the electrical oscillations of the sample holder. If the bunch frequency is 78 kHz, there is enough time for these oscillations to decay before the next bunch arrives, even without the ferrite.

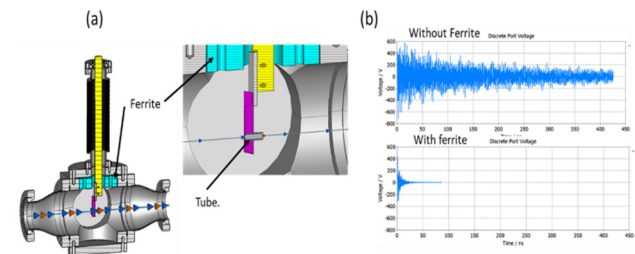


Figure 8: Simulation of the electrical response for the diamond detector system. (a) 3D model of detector system, tube was used to simulate the interaction of the beam with the target; (b) Detector voltage plots with respect to ground for 5 nC, 100 ps FWHM bunches, with and without ferrite.

### CeC BEAM TEST

The DBPD was installed close to the beam dump of the CeC diagnostic beam line to minimize radiation from scattered electrons impacting the beam pipe. CeC beam test (about 30 pC per bunch) was performed at 5 and 78 kHz repetition rates. Diamond sensor was moved into the beam pipe line from a fully retracted position, inserted into the beam core for 20 sec, and retracted back. Thus, only half of the beam profile was measured. Digital electrometers used for transient current measurements (2 x F460, 8 total channels, 16 bit, 250 kHz, Pyramid Tech. Cons.) were not

synchronized with electron beam pulses which resulted in multiple missed pulses. Acquisition time constant of the electrometers was 0.1 s. Electrical bias of the diamond sensor was 0 V, and diamond thickness was 150  $\mu\text{m}$ .

The diamond detector was fully operational under its full insertion into the 78 kHz CW CeC beam core for up to 20 sec. Transient currents (up to 2000 pA) were detected from the horizontal electrode and all six vertical electrodes. The horizontal beam profiles measured by vertical electrodes and vertical beam profile measured by horizontal electrode, are shown in Figs 9 (5 Hz) and 10 (78 kHz). The vertical beam profile at 78 kHz shows an approximately 3 mm wide core well corresponding to the expected the CeC beam width (see Table 1), but it shows very narrow vertical profile at 5 Hz. The horizontal beam profile demonstrates rather unusual double beam cores with second core at channel 4 (5 Hz) and channel 3 (78 kHz). Both observed effects, a narrow vertical beam profile at 5 Hz and double corers, could be the artefacts resulting from low signal intensities at 5 Hz due to the poor signal synchronization, and different strip's sensitivity to the radiation. Thus, the strip's sensitivity to the electron beam must be calibrated before the measurements, e.g. by sweeping the standard narrow radiation beam onto each strip and comparing their responses. Additional tests with higher detector sensitivity (the use of bias voltage will increase the detector signals > 10 times), proper synchronization, and more detector's strips may clarify the observed beam profile data.

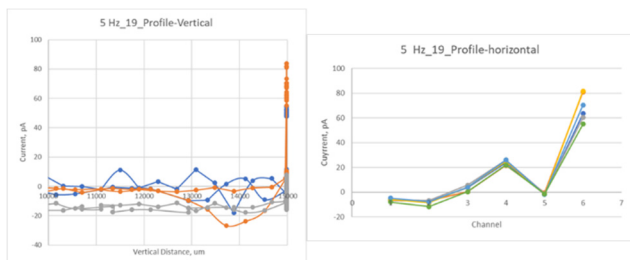


Figure 9: Vertical (left) and horizontal (right) beam profiles for pulsed (5 Hz) CeC beam mode.

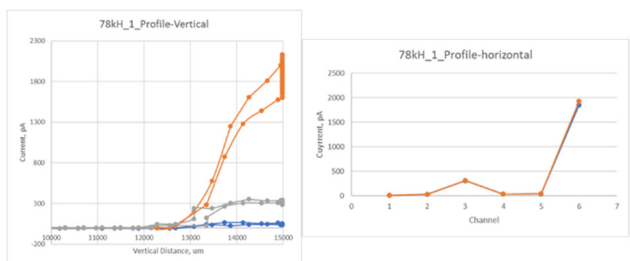


Figure 10: Vertical (left) and horizontal (right) beam profiles for CW (78 kHz) CeC beam mode.

Note, that a 20 s long insertion of diamond sensor into the CeC beam core produced high levels of secondary radiation likely caused by the electron beam interactions with the diamond sensor itself and/or produced by scattered electrons interacting with downstream sections of the beam pipe.

## CONCLUSIONS

- For the 78  $\mu\text{A}$  CW CeC beam, the steady state condition with a maximum temperature of about 100  $^{\circ}\text{C}$  is reached at about 10-20 sec after the beam is turned on. At the maximum actuator speed, the total insertion/removal time of the sensor could be as small as 180 ms. In this case the maximum temperature of 30  $^{\circ}\text{C}$  occurs at about 40 ms and then returns to the ambient within 5 s.
- For the 35.5 mA CW LEReC beam, at the maximum actuator speed the maximum temperature of about 370  $^{\circ}\text{C}$  occurs at about 140 ms and then, similarly to the CeC, returns to the ambient within 5 seconds.
- The first prototype of a fast scanning diamond beam profile detector suitable for invasive high power CW electron beam core profile measurements in transmittance mode was developed and successfully tested with pulsed (5 Hz) and CW (78 kHz) CeC beams.
- Transient currents from the multi-strip diamond detector were measured with fast digitizing electrometers and XY beam profile can be obtained in one scan.
- The limitation imposed by the diamond detector installation close to the beam dump of the CeC beam line to minimize radiation from scattered electrons impacting the beam pipe needs to be considered for any future applications.
- Scattering of the electrons in the diamond sensor causes most of the beam to be lost on the walls of the beam pipe over a few meters downstream of the detector. The beam interruption and excessive amount of secondary radiation produced could be mitigated in the future by much shorter insertion times or by avoiding full insertion when only beam halo measurements are of interest. The secondary radiation from diamond sensor can be effectively shielded as well.

## REFERENCES

- [1] A.V. Fedotov *et al.*, "Experimental demonstration of hadron beam cooling using radio-frequency accelerated electron bunches", *Phys. Rev. Lett.*, vol. 124, p. 084801, 2020.
- [2] V. Litvinenko *et al.*, "Coherent Electron Cooling Experiment at RHIC: Status and Plans", in *Proc. 12th Workshop on Beam Cooling and Related Topics (COOL'19)*, Novosibirsk, Russia, Sep. 2019, pp. 35-40.  
doi:10.18429/JACoW-COOL2019-TUZ01
- [3] S. Seletskiy *et al.*, "Status of the BNL LEReC Machine Protection System", in *Proc. 7th Int. Beam Instrumentation Conf. (IBIC'18)*, Shanghai, China, Sep. 2018, pp. 249-252.  
doi:10.18429/JACoW-IBIC2018-TUPA17
- [4] W. Trischuk, "Diamond Particle Detectors for High Energy Physics (RD42)", *Nucl. Particle Phys. Proc.*, vol.273-275, pp.1023-1028, 2016.
- [5] E. Muller, "Transmission-mode diamond white-beam position monitor at NSLS", *J Synchrotron Radiat.*, vol. 19, pp. 381-387, 2012.
- [6] K. Desjardins, M. Bordessoule, and M. Pomorski, "X-ray position-sensitive duo-lateral diamond detectors at SOLEIL", *J. Synchrotron Rad.*, vol. 25, pp. 399-406, 2018.

- [7] P. Bergonzo, D. Tomson, and C. Mer, “CVD diamond-based semi-transparent beam position monitors for synchrotron beamlines: preliminary studies and device developments at CEA/Saclay”, *J. Synchrotron Rad.*, vol. 13, pp. 151-158, 2006.
- [8] J. Bohon, E. Miller, and J. Smedley, “Development of diamond-based X-ray detection for high-flux beamline diagnostics”, *J. Synchrotron Rad.*, vol. 17, pp. 711–718, 2010.
- [9] H. Aoyagi *et al.*, “Pulse-mode measurement of electron beam halo using diamond-based detector”, *Phys. Rev. ST Accel. Beams*, vol. 15, p. 022801, 2012.